Ann. Geophys. Discuss.,
https://doi.org/10.5194/angeo-2019-90-AC1, 2019

Annales Geophysicae Discussions
Open Access
EGU

Interactive comment on "MMS observations of energetic oxygen ions at the low-latitude duskside magnetopause during intense substorms" *by* Chen Zeng et al.

Chen Zeng et al.

czeng@spaceweather.ac.cn

Received and published: 30 August 2019

Dear reviewer: We are very grateful to your comments for our manuscript. According to your advice, we amended the relevant part in the manuscript. The one-to-one responses are the following.

Comment 1: Line 138: The authors should clarify the information on which instrument dataset was used for each data product. Were the moments shown in Figure 2c-2e recalculated from the FPI distribution functions? Or are they the default moments calculated over the full FPI energy range?

Printer-friendly version

Discussion paper

Response: Thanks for the referee's kind advice. We should have clarified the dataset information in Figure 2 on which instrument was used. So I added detailed information about dataset we used to the description of Figure 2. The plasma moments (e.g. Ion parallel and perpendicular temperatures, ion, and electron number densities and ion velocity) from FPI shown in Figure 2c-2e are all from MMS L2 data products. They are default moments calculated over the full FPI energy range from 10 eV to 30 keV. But the O+ density shown in Figure 2f is recalculated from HPCA distribution functions at energies from 1 to 40 keV. From the O+ fluxes shown in Figure 2j, there still exists a large number of fluxes below 1 keV in the magnetosheath. This part of O+ fluxes is fake and contamination from high proton fluxes. So we consider the number density of O+ at energies from 1 to 40 keV is more appropriate to represent the true O+ in the magnetopause. While the H+ density (over the full HPCA energy range) from L2 data products are used in Figure 2f. The magnetic and electric fields in GSM are from FGM and EDP, respectively. The last four panels of Figure 2 show the omnidirectional differential fluxes of four individual ion species, H+, O+, He+, and He++ measured by HPCA, respectively.

Comment 2: Line 140 (Figure 2f): The calculations performed to derive the >1 keV O+ density need to be described to inform the reader how the HPCA energy ranges were specified for those calculations. If a software package was used, then details of the software package and a citation to it should be included. The >1keV H+ density could also be plotted in this figure panel.

Response: Thanks for the referee's good suggestion. As mentioned before, the >1 keV O+ density (shown in Figure 2f) recalculated from the HPCA distribution functions at energies from 1 to 40 keV. As your suggestion, I also plotted the H+ density over the full FPI energy range from 10 eV to 40 keV in Figure 2f for better comparison. Because of H+ measurements from HPCA is accurate and the H+ mean energy in the magnetosheath is typically 0.3 keV, so we used the H+ density (over the full HPCA energy range) from L2 data products. These O+ density calculations are used

The Space Physics Environment Data Analysis System (SPEDAS) software package. More details about SPEDAS can be found in Angelopoulos et al. (2019) and cited as (Angelopoulos, V., Cruce, P., Drozdov, A. et al. Space Sci Rev (2019) 215: 9. https://doi.org/10.1007/s11214-018-0576-4). We also cited this paper in our revised manuscript (see Line 111-113).

Figure 2. The energetic O+ are observed at the magnetopause during an intense substorm on 03 October 2015 by MMS 4. From top to bottom are (a) the magnetic field three components, Bx (blue line), By (gree line), Bz (red line) and the total magnitude Bt (black line), (b) the electric field three components, Ex (blue), Ey (gree) and Ez (red), (c) Ion parallel (red) and perpendicular(black) temperatures, (d) The number density of ion (green) and electron (blue), (e) three components of the ion velocity, (f) number density of H+ (over the full HPCA energy range) and O+ (at energies from 1 to 40 keV), (g) electron omnidirectional differential energy fluxes, (h) ion omnidirectional differential energy fluxes, (i) to (l) present omnidirectional differential particle fluxes of H+, O+, He+, and He++, respectively. The Geocentric Solar Magnetospheric (GSM) coordinate system is adopted. The thick bars at the top of the panel represent different regions encountered on this magnetopause crossing event. The orange and blue bars represent the magnetosheath and the magnetosphere, respectively. The green bar represents the magnetopause boundary layer. The black horizontal line in figure 2j is at 1 keV and the O+ contamination from high H+ fluxes is indicated by the red box. The FPI data in Figure 2(c-e) and (g-h) are from FPI L2 data product and in the fast mode.

Comment 3: Line 158-164: The magnetopause identification criteria are not very convincing. Recommend carefully defining these criteria, as all statistics are derived based on the magnetopause identification. Recommend the authors review identification criteria used in previous works. For example, Haaland et al. (2016) and (2019) describe magnetopause observations by Cluster and THEMIS: Haaland, S., Reistad, J., Tenfjord, P., Gjerloev, J., Maes, L., DeKeyser, J., Maggiolo,R., Anekallu, C., and Dorville, N. (2014), Characteristics of the flank magnetopause:Cluster observa-

tions, J. Geophys. Res. Space Physics, 119, 9019–9037,doi:10.1002/2014JA020539. Haaland, S., Runov, A., Artemyev, A., & Angelopoulos, V. (2019). Characteristics of the flank magnetopause: THEMIS observations. Journal of Geophysical Research: Space Physics, 124, 3421–3435. https://doi.org/10.1029/2019JA026459. Paschmann et al. (2018) describe magnetopause identification and observations by MMS: Paschmann, G., Haaland, S. E., Phan, T. D., Sonnerup, B. U. Ö., Burch, J. L., Torbert, R. B., et al. (2018). Large-scale survey of the structure of the dayside magnetopause by MMS. Journal of Geophysical Research: Space Physics, 123, 2018–2033. https://doi.org/10.1002/2017JA025121.

Response: Thanks for the referee's kind suggestion and well recommend. We read the papers your recommended and found they did detailed work for magnetopause identification. It deepens my understanding of the flank magnetopause characteristics and helps me identifying the magnetopause more convincing. In this study, we mainly focus on the O+ in the dusk flank magnetopause boundary layer. According to the magnetic field, B is about 40 nT and O+ temperature, T is about 10 keV in this study, we can draw the O+ gyroradius is about 1020 km. From Haaland et al. (2014), the flank magnetopause thickness varies from 150 to 5000 km with a median thickness of around 1150 at dusk. Thus the gyroradius of ten keV O+ is comparable to magnetopause thickness. In that situation, O+ will show the finite Larmor radius effects and the MMS detect partial gyro motion in the magnetopause. For acquiring complete O+ distribution functions, we need to measure O+ in more large spatial scales. So in this study, we focus on the magnetopause boundary layer judgment. The magnetopause boundary layers are identiïňĄed here primarily through plasma ïňĆuxes and moments. The low-latitude boundary layer (LLBL) on the magnetospheric side of the magnetopause current layer and the magnetosheath boundary layer (MSBL) on the magnetosheath side of the magnetopause current layer can have densities and temperatures between that of the magnetosphere and magnetosheath. Ion jets are also signatures of passing through the magnetopause boundary layers. In this study, the separatrix between the magnetosheath and the magnetopause boundary layer is determined by the appear-

ance of the magnetospheric electron, as the first black solid line in Figure 2 shown. Similarily, the separatrix of the magnetosphere and the magnetopause boundary layer is determined by the magnetosheath electron disappearance, as the second solid line in Figure 2 shown. The revised details can be found in Line 182-212.

Comment 4: Line 180: More details are needed to describe how the mean values of the H+ and O+ fluxes and densities were calculated.

Response: Thanks for the referee's kind advice. First, we determine the time interval of the magnetopause boundary layer crossings in each event. For example, on 03 October 2015 event, MMS 4 traversed the duskside magnetopause boundary layer from 15:25:10 to 15:36:50 UT judged by the typical characteristics in this region as mentioned before. Then, the H+ and O+ fluxes and densities were average during this time interval. We also give the error bars indicating 95% confidence intervals. We think these mean values represent the H+ and O+ fluxes and densities in the magnetopause boundary layer. See Line 218-222.

Comment 5: Line 184: A more detailed description of how the substorm phase (i.e. expansion phase or recovery phase) was defined based on AE index is needed. The authors should use Figure 1 AE index to aid in their description.

Response: Thanks for the referee's suggestion. We should give more details to clarify how we define the substorm phase according to substorm indices, such as AU, AL, and AE index. First, we determined the time interval of the magnetopause boundary layer crossings in each event. Then, see how the substorm indices vary during that interval from the OMNI data. As Figure 1 shown, the time interval of the magnetopause boundary layer crossing is marked by the two blue dashed lines. As we know, the AE index is defined as AE=AU-AL. Generally, the substorm onset time is characteristic by the AL index starts to significantly decrease and the AE index significantly increase. During the substorm expansion phase, the AL index will decrease significantly. The interval of the AL index decrease from onset to its minimum is defined as the substorm

expansion phase. Then it starts to increase and the interval of the AL index increase from the minimum to the quiet time level is regarded as the substorm recovery phase. In our event, the MMS4 crossed the magnetopause boundary layer from 15:25:10 to 15:36:50 UT on 3 October 2015. From Figure 1f, the AL index reached its minimum ∼-750 nT and AE index reach the peak ∼1000 nT at about 15:20 UT, then it started to increase to ∼ -200 nT at the rest time of interest. The two blue dashed lines indicate the time interval of the magnetopause boundary layer crossing. According to the variation and peak value of the AU, AL and AE index in Figure 1e to 1g. The magnetopause boundary layer crossing occurred during the recovery phase of this intense substorm.

Figure 1. The three components IMF Bx, By, Bz, solar wind dynamic pressure, as well as AU, AL, and AE index from CDAweb OMNI data.

Comments 6: Line 202-209: Several narrow energy ranges used for comparing the O+/H+ density ratio are noted. It is important to describe for the reader how these energy ranges were used in the density ratio calculations. In addition, a description of why these energy ranges were chosen should be included. Did the authors consider calculating the density ratio for all energies >1 keV instead of calculating the ratios over individual energy ranges? A comparison of density ratios using both methods may be helpful to decide which method to use. Such procedural information on which analysis methodology was chosen could be included in an appendix.

Response: Thanks for carefully evaluating this manuscript and kind suggestions. The description in Line 202-209 is not accurate and it appears that the referee has some misunderstanding on what we did. In this study, we calculate the O+/H+ density ratio (as Figure 4b shown). The O+ density calculated at energies from 1 to 40 keV, but the H+ density (over the full HPCA energy range) from L2 data products are used. In order to realize in which individual energy ranges the O+ abundance (O+/H+) varies obviously on AE index and solar wind parameters. We calculated the particle fluxes ratio at several individual energy ranges (as Figure 4c shown). Since the energy channel range of HPCA for H+ and O+ is the same, so the fluxes ratio are defined as the ratio

between their fluxes, We also give the error bars indicating 95% confidence intervals.

Comments 7: Line 218-248: Figures 5, 6, 7 all show comparisons of the O+/H+ density ratio. After addressing the previous comment on Line 202-209 on why separate narrow energy ranges were chosen instead of using a broad energy range, the authors may need to revise panel (b) of these three figures. For example on Line 240: Are the O+ and H+ densities referred to in this section calculated from one of the energy ranges discussed in Line 202-209? Greater detail and explanation are needed.

Response: It may be our inaccurate descriptions result in the referee's misunderstood. Figure 4b 5b, 6b, 7b show the O+/H+ density ratio used the broad energy range (as mentioned in Response to comment 6). While Figure 4c, 5c, 6c, 7c show the O+/H+ fluxes ratio at several individual energy ranges. We didn't calculate the O+ or H+ density from one of the energy ranges discussed in Line 202-209. So this relevant part of the description has been amended in my revised manuscript.

Comments 8: Line 254-256: After addressing the above comments on how the ion densities were calculated, the authors should briefly address whether these comparisons of density across missions are relevant. For example, if the O+ density (calculated over defined HPCA energy range) is higher than seen by Cluster (calculated in what energy range and using which instrument?), what does this mean? Were the instrument energy ranges equivalent or similar? Otherwise, the direct comparison may not be meaningful.

Response: Thanks for the referee's good evaluation and kind suggestion. This comment is very important. From Line 254-256, we can't exclude the reason that Bouhram et al., 2005 used somewhat different energy range for O+ observations result in lower O+ density in their study than mine. The direct comparison can't be meaningful. In this study, the O+ density calculated using HPCA distribution functions at energies from 1 to 40 keV, but Bouhram et al., (2005) used CODIF distribution functions at energies from 3 to 40 keV to avoid contamination from high H+ fluxes. The composition and

distribution function (CODIF) analyzer on the Cluster that measures 3-D distributions of the major ion species over the energy range 30–40000 eV. This contrast study is not rigid in this study, so we removed the relevant part in our revisited manuscript.

Comments 9: Line 305: Since 31 events are not a large number, recommend the authors produce a table to list the dates and times of each of these events so that others in the space science community can also investigate the events for follow-on studies. Such a table could go in an appendix.

Response: Yes, this is a good suggestion. I have prepared such a table to list the dates and times of each of these events for follow-on studies in an appendix (see the attachment).

Comments 10: All the references in the manuscript need to be checked. For example, all the MMS instrument papers were referenced but do not appear in the references list. It is likely any other references have been missed. It is likely many other references have been missed. Line 106: Pollock et al. (2016) is referenced but does not appear in the references list Line 105: Russell et al. (2016) is referenced but does not appear in the references list Line 104: Ergun et al. (2016) is referenced but does not appear in the references list Line 104: Lindqvist et al. (2016) is referenced but does not appear in the referenceslist Line 107: Young et al. (2016) is referenced but does not appear in the references list

Response: Thanks for the referee's kind remind and carefully evaluating this paper. This stupid mistake should have avoided in the manuscript submission. We added the MMS instrument papers citations in the references list. We also checked carefully all the references in the manuscript to make sure all the citations in the references list. The other spelling and syntax errors have been checked and corrected. We acknowledge the reviewer's comments and suggestions very much, which are valuable in improving the quality of our manuscript.

Please also note the supplement to this comment:
https://www.ann-geophys-discuss.net/angeo-2019-90/angeo-2019-90-AC1-supplement.pdf

---

Interactive comment on Ann. Geophys. Discuss., https://doi.org/10.5194/angeo-2019-90, 2019.

Printer-friendly version

Discussion paper

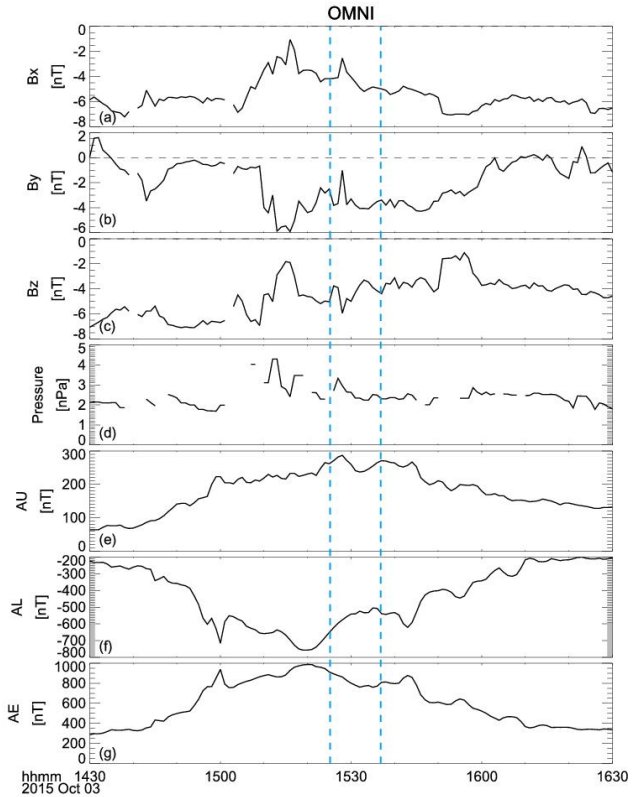

Fig. 1. The three components IMF Bx, By, Bz, solar wind dynamic pressure, as well as AU, AL, and AE index from CDAweb OMNI data

Printer-friendly version

Discussion paper

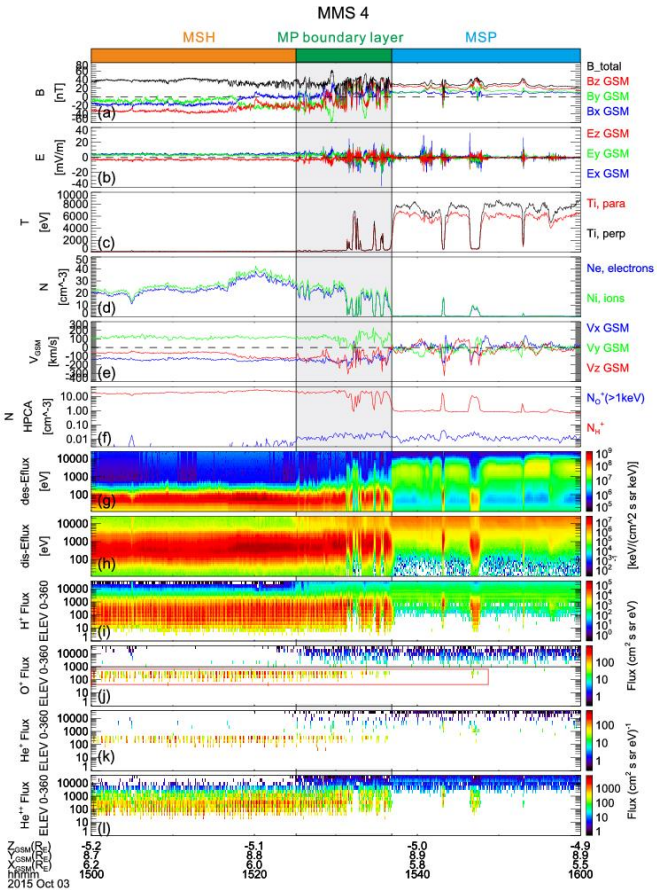

Fig. 2. The energetic O+ are observed at the magnetopause during an intense substorm on 03 October 2015 by MMS 4

Printer-friendly version

Discussion paper